

European Radiology

© Springer-Verlag 2004

10.1007/s00330-004-2521-z

Cardiac

Visualisation of non-invasive coronary bypass imaging 4-row vs. 16-row multidetector computed tomography

M. Fawad Khan¹ , Christopher Herzog¹, Kai Landenberger¹, Adel Maataoui¹, Sven Martens², Hanns Ackermann³, Anton Moritz² and Thomas J. Vogl¹

- (1) Institute for Diagnostic and Interventional Radiology, Johann Wolfgang Goethe University, Theodor-Stern-Kai 7, 60590 Frankfurt/Main, Germany
- (2) Department for Thoracic and Cardiovascular Surgery, Johann Wolfgang Goethe University, Theodor-Stern-Kai 7, 60590 Frankfurt/Main, Germany
- (3) Institute for Epidemiology and Medical Statistics, Johann Wolfgang Goethe University, Theodor-Stern-Kai 7, 60590 Frankfurt/Main, Germany

 M. Fawad Khan

Email: fawad@gmx.de

Phone: +49-69-63017277

Fax: +49-69-63017258

Received: 15 June 2004 **Revised:** 25 August 2004 **Accepted:** 30 August 2004 **Published online:** 15 October 2004

Abstract The purpose of this study was to investigate the image quality of coronary artery bypass graft visualization in 4- and 16-row multidetector CT using multiple imaging reformations. *Material and Methods:* One hundred sixteen patients underwent CT examination of the heart after receiving CABG. Group A ($n=58$) received 4-row MDCT; group B ($n=58$) received 16-row MDCT. Various bypass types such as LITA to LAD and venous grafts to the RCA and RCX were included in the study. A five-point Likert scale was used to grade image quality. Each bypass was reviewed under different imaging reformations: thin slab maximum intensity projection (MIP thin), multiplanar reformation (MPR) and volume rendering technique (VRT). Special attention was paid to the delineation of the distal anastomosis. Interobserver correlation

was determined. *Results:* From 289 bypass grafts examined, 279 (96.54%) were classified as patent and 10 (3.46%) as not patent. Except for the distal anastomosis, 16-row MDCT showed significantly better results for all segments of bypasses. Comparison of reformations within group A and B showed that MIP thin ($P<0.05$) and VRT ($P<0.05$) displayed better visualization as compared to MPR. *Conclusion:* Significantly better imaging of all bypass types is possible using 16-row MDCT as compared to 4-row MDCT. Assessment of the distal anastomosis yields no difference between 4- and 16-row technology.

Keywords Coronary arteries bypass graft - MDCT angiography - Cardiac MDCT

Objective

Coronary artery bypass surgery is a key foundation in the therapy of coronary artery disease (CAD). In 2001, 77,000 coronary bypass procedures were performed in Germany [1]. However, the patency rate of bypass grafts is limited. Eleven days postoperatively, 1.3% of left internal thoracic artery (LITA) grafts are occluded [2]. One year after surgery, 3.4–5.7% of all arterial grafts are not patent anymore [3]. In venous grafts, the postoperative follow-up yields even worse results.

In women 16.7% and in men 12.4% have occluded venous bypass grafts 1 year after surgery [3]. One year after surgery, the postoperative mortality is 2.8% and the myocardial infarction (MI) rate reaches 4% [4]. Three years after surgery, 20–30% of all bypass grafts are occluded [5].

Sites of anastomosis are particularly prone to occlusion [4, 6]. In asymptomatic CABG patients, an invasive procedure such as coronary angiography for assessment of graft patency cannot be recommended in general because of its evident risks [7]. Moreover, the inconveniences for the patients as well as the economic burden have fueled the quest to find an alternative, non-invasive method to close this diagnostic gap. Multidetector row CT (MDCT) for non-invasive coronary bypass graft imaging and assessment of graft patency is an emerging technique bearing the potential to close this gap. In prior studies, using 4-row MDCT evaluation of the distal anastomosis, if possible at all, is very challenging and exhibits a major limitation in using 4-row MDCT technology [8, 9]. In 16-row MDCT, temporal resolution is further improved and nearly isotropic in-plane and z resolution is achieved. As a consequence, new isotropic voxeling leads to higher resolutions in various imaging planes. But does this also result in better image quality?

In this study, we examined the outcome of 16-row multidetector CT technology as compared to 4-row MDCT on CABG imaging, using visualization techniques such as multiplanar reformations (MPR), maximum intensity projection (MIP) and volume-rendered technique (VRT).

Materials and methods

Patients

We studied retrospectively 116 patients (92 men and 24 women) who had undergone cardiac multidetector row CT over a 2-year period. All patients had undergone CABG surgery before being scanned. Patients in group A were scanned in the 1st year of this study. Patients in group B were scanned in the 2nd year of this study. None of the patients suffered from angina pectoris or had any indication of myocardial ischemia. Patient comorbidity is listed in Table [1](#).

Table 1 Patient comorbidity

	Group A	Group B	<i>P</i> value
Arterial hypertension	51 (88%)	49 (85%)	n.s.
Hyperlipidemia	29 (50%)	29 (50%)	n.s.
Obesity	20 (34%)	19 (33%)	n.s.
Diabetes mellitus	9 (16%)	12 (21%)	n.s.
History of smoking	15 (26%)	20 (35%)	n.s.
Single vessel disease	2	2	n.s.
2-vessel disease	31	29	n.s.
3-vessel disease	25	27	n.s.

n.s. not significant ($P>0.05$).

Group A ($n=58$) received 4-row MDCT (Somatom Plus 4 VolumeZoom WIP Version VA 20; Siemens, Forchheim, Germany) and group B ($n=58$) received 16-row MDCT (Sensation 16, Siemens, Forchheim, Germany). The average time between surgery and the CT exam was 5.82

± 1.1 days (range 3–10 days) for group A and 5.68 ± 1.3 days (range 3–11 days) for group B; mean patient age was 67.69 ± 7.44 years (range 47–86 years) for group A and 68.05 ± 6.33 years for group B (range 42–81 years); mean heart rate was 76.09 ± 12.62 beats per minute (bpm) (range 54–122 bpm) for group A and 83.74 ± 21.19 bpm (range 53–198 bpm) for group B ($P > 0.05$).

All patients were enrolled in the study approved by the institutional review board and had previously signed informed consent. The number of bypass grafts in each patient ranged from one to five grafts. A total number of 289 grafts (group A: 149; group B: 140), of which 180 venous (group A: 93; group B: 87) and 109 arterial (group A: 56; group B: 53) grafts were examined. Bypass types such as LITA to LAD (109) [(arterial grafts)] and venous grafts to the RCA (91), RCX (89) were examined. Bypass numbers and bypass types are listed in detail in Table 2.

Table 2 Bypass numbers and bypass types

LITA–LAD	109	Arterial	Distal anastomosis in the distal LAD
ACVB–RCA	91	Venous	Distal anastomosis in the distal RCA
ACVB–RCX	89	Venous	Distal anastomosis in the distal RCX
Total	289		

CT imaging

In both groups, all CT scans were obtained by using a multidetector row MDCT scanner. In group A, a 4-row MDCT (Somatom Plus 4 VolumeZoom WIP-version VA 20; Siemens, Forchheim, Germany) was used. In group B, a 16-row MDCT (Sensation 16, Siemens, Forchheim, Germany) was used. Patients with heart rates greater than 70 bpm previously received a short-lasting beta-blocker (esmolol hydrochloride, Brevibloc; Baxter, Unterschleisheim) administered at 10 mg per 10 kg of body weight to obtain rates of 60 bpm or less. However, as medical treatment often did not produce any effect, in some patients, heart rates higher than 70 bpm were observed. Each patient underwent contrast-enhanced examinations.

In group A (4-row MDCT), scanning parameters were 120 kV and 300 mAs, 500-ms rotation time, 4×1.0 -mm section collimation and 1.5-mm table feed per rotation for the contrast-enhanced series. All patients in group A received 140 ml of a non-ionic contrast medium (Ultravist; Schering, Berlin, Germany) infused through an 18-gauge intravenous antecubital catheter at a flow rate of 3.5 ml/s. Start delay was calculated with a test bolus placed in the ascending aorta; 30 ml of contrast medium was administered at a flow rate of 3.5 ml/s. Scan range was in a craniocaudal direction from the distal ascending aorta to the diaphragm. Mean scan time was 38 ± 7 s.

In group B (16-row MDCT), scanning parameters were 120 kV and 500 mAs, 420-ms rotation time, 16×0.75 -mm section collimation and 2.8-mm table feed per rotation for the contrast-enhanced series. All patients in group B received 140 ml of a non-ionic contrast medium (Ultravist; Schering, Berlin) and 40 ml isotonic saline solution (Isotonic NaCl 0.9%, B. Braun Melsungen, Inc., Melsungen, Germany) in a row using a double head injector [10] (Injektron CT 2, Medtron, Inc., Saarbruecken, Germany) infused through an 18-gauge intravenous antecubital catheter at a flow rate of 3.5 ml/s. CareBolus technique (Siemens, Erlangen, Germany) was used to determine the optimal scan start in placing a ROI in the ascending aorta and setting the density threshold on 140 HU. Scan range was in a craniocaudal direction from the distal ascending aorta to the diaphragm. Mean scan time was 19 ± 7 s. Because of the 180° linear interpolation, exposure time was minimized to 210 ms in group B and to 250 ms in group A.

Image reconstruction

Image reconstruction was performed by using retrospective ECG gating, a technique that allowed continuous image reconstruction from volume data sets during any phase of the cardiac cycle [11, 12]. The following reconstruction parameters were used in group A (4-row MDCT): 220-mm field of view, a medium soft tissue kernel, 1.25-mm effective slice thickness and 0.5-mm increment for the contrast-enhanced series. In group B (16-row MDCT), reconstruction parameters were as mentioned for group A, but differed as slice thickness was lowered to 1 mm; the increment stayed at 0.5 mm.

The adaptive cardiac volume reconstruction algorithm, standard software provided with the software package of the CT scanner, was used for image reconstruction. This algorithm combined two different reconstruction algorithms, depending on the heart rate: single segmental reconstruction (SSR) [≤ 65 bpm] and adaptive-segmental reconstruction (ASR) [≥ 65 bpm]. For SSR only data from one rotation are required for image reconstruction; for ASR data from at least two rotations are required for the reconstruction of each 1.25-mm slice (group A)/1-slice mm (group B) [13]. In group A, temporal resolution for SSR constantly was 250 ms and in group B, 210 ms. For ASR, temporal resolution varied according to the heart rate and ranged between 125 and 250 ms for group A and 110 and 220 ms for group B [14]. Considering basic cardiac physiology, image reconstruction is performed best in the late systole (i.e., ascending T wave) and the late diastole (i.e., beginning of the P wave) [14]. Consequently, each data set was reconstructed at multiple time points within this interval, differing from each other by 50 ms [15]. The number of possible reconstruction time points per patient ranged between six (elevated heart rate) and ten (low heart rate), depending on the length of the TP interval (time between the T wave and the P wave). The TP interval decreases as heart rate increases. At each time point, image reconstruction was performed antegrade and absolute (i.e., in 0, 50, 100, 150, 200, etc., ms) in relation to the R peak. Subsequently for each patient and each bypass graft separately, a single reconstruction was determined that displayed the fewest motion artifacts in the segment or anastomosis to be examined and therefore made a proper image interpretation possible [16–21].

Image reformation and evaluation

For both groups alike, evaluation of the bypass grafts was performed by dividing each bypass graft into three segments: a proximal, middle and distal segment. In addition, the sites of proximal and distal bypass anastomosis were evaluated. After initial blinding by a technician, each dataset was evaluated by two independent observers (M.F.K., K.L.) separately.

Images were evaluated with three reformation techniques in both groups: MIP thin, MPR and VRT. Each visualization technique was examined in separate readings. To avoid bias from previous readings, a 7-day time gap between readings was kept. Each observer did the reformations for evaluation by himself.

For patients in both groups, evaluations were performed on a separate workstation (Leonardo, Siemens, Inc., Erlangen, Germany) with a 512×512 matrix size.

Observers were asked to grade image quality on a five-point Likert scale (1, excellent; 2, good; 3, moderate; 4, poor; 5, not visible) for every segment as well as the sites of anastomosis. Grading criteria were as follows:

- (1) Delimitation between the vessel and surrounding structures
- (2) Blurring of the segments course caused by artifacts
- (3) Differentiation between vascular lumen and wall—not for VRT.

Observers were instructed to judge each of the three grading criteria according to the five-point Likert scale from which an average grade was calculated. Depending on the image quality and complexity of the CABG surgery, the evaluation lasted between 40 and 60 min per patient. Each observer rated each patient and reformation technique.

Statistical analysis

Statistical analysis was carried out using the StatView software package (Abacus Concepts, Berkeley, CA). Data are presented as mean \pm standard error. The Wilcoxon matched pairs test was used to compare different reformations within a group as well as to compare corresponding reformations between groups. To assess interobserver correlation, the Spearman-Rank test was used. Differences were considered significant when the *P* value was below 0.05.

Results

From 289 bypass grafts examined, 279 (96.54%) were classified as patent and 10 (3.46%) as not patent. All total occlusions were observed in the proximal anastomosis, i.e., in ACVB to RCx and ACVB to RCA grafts. No subtotal plaque formation could be reported in any segment evaluated. For the different bypass graft types, the following results can be reported in comparison of both groups.

In LITA to LAD bypasses, 16-row MDCT technology yielded better visualization in the total course as well as the proximal, middle and distal course of the bypass graft ($P < 0.05$) [(Fig. [1](#), 4-row vs. 16-row)]. We cannot report a better visualization for the distal anastomosis in LITA to LAD grafts ($P > 0.05$) [(Fig. [2](#), 4-row vs. 16-row)].

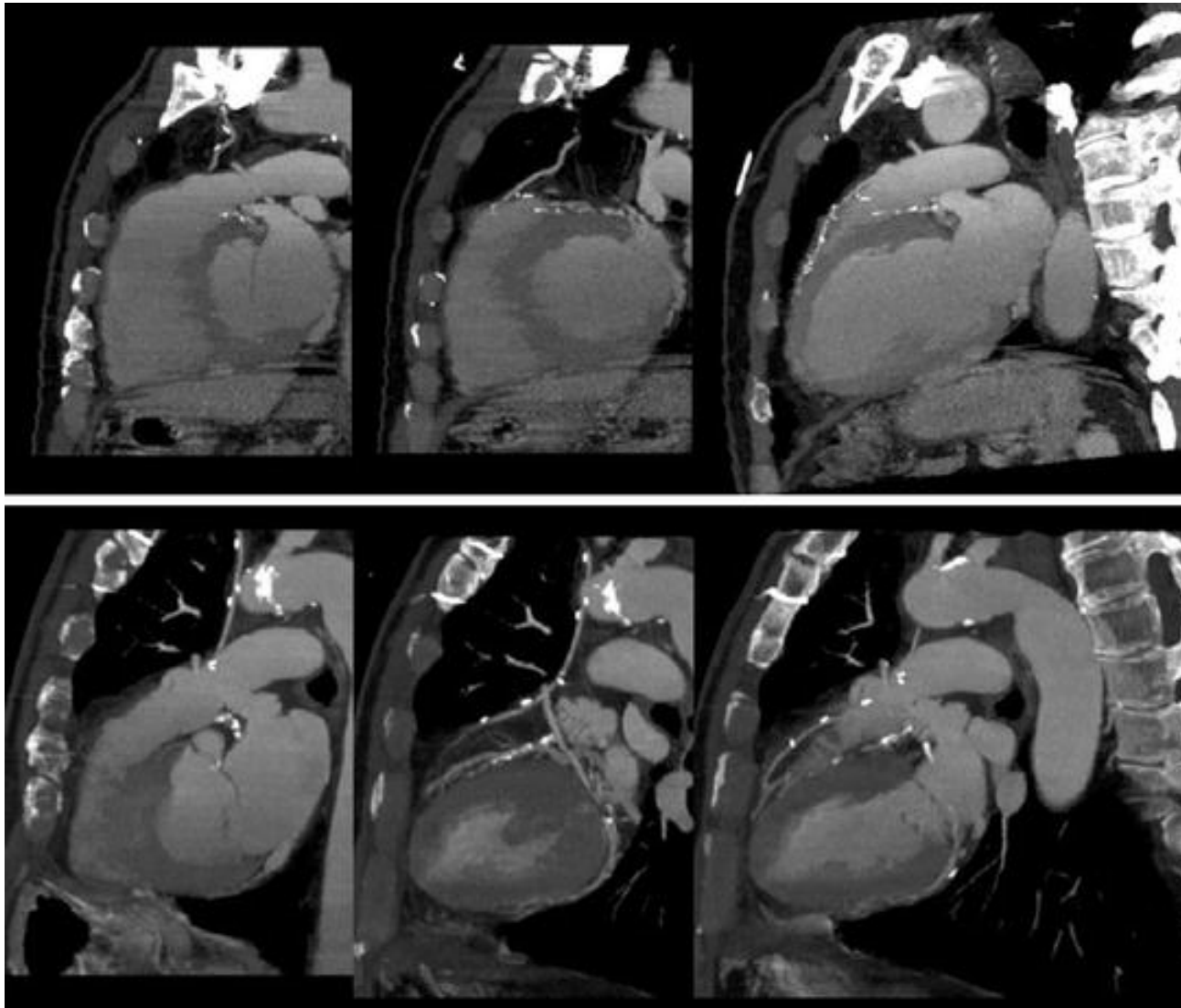


Fig. 1 Four-row (*upper row images*) vs. 16-row MDCT (*lower row images*) LITA to LAD bypass in the proximal, middle and distal course

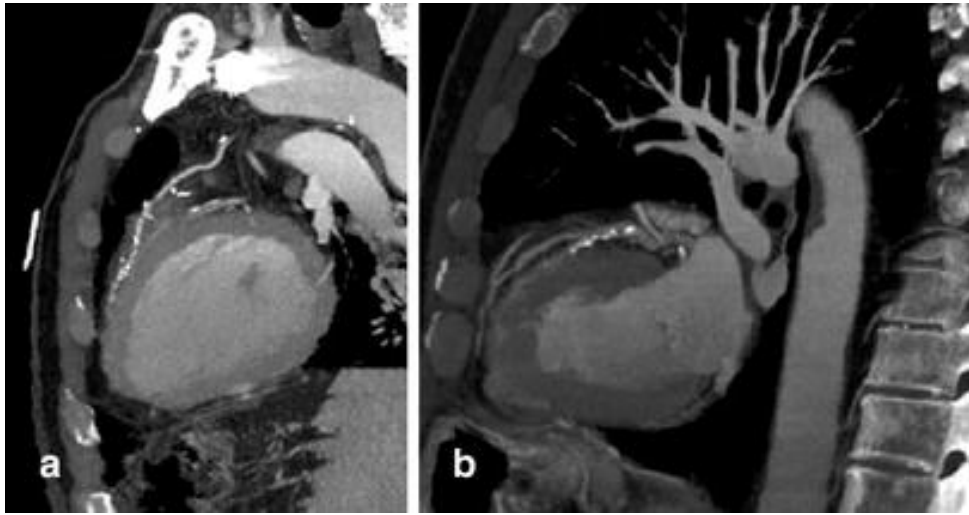


Fig. 2 Four-row (*left image*) vs. 16-row (*right image*) MDCT LITA to LAD bypass at the distal anastomosis

In ACVB to RCX bypasses, 16-row technology also provided better visualization of the bypass graft ($P<0.05$) except for the distal anastomosis, which did not show a significant improvement ($P>0.05$) [(Fig. 3, 4-row vs. 16-row)]. The proximal site of anastomosis, not existent in LITA to LAD grafts, could be better displayed as well ($P<0.05$).

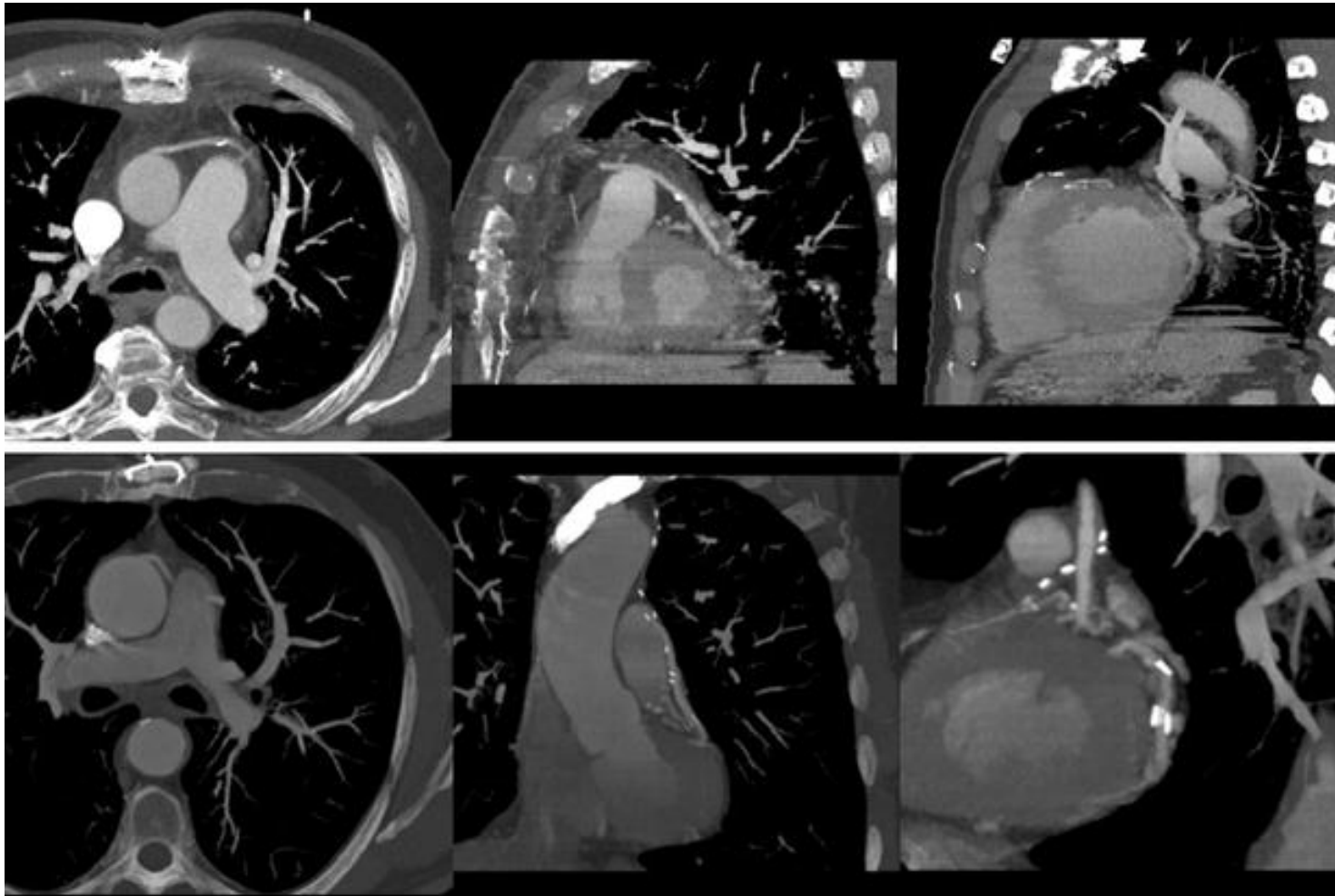


Fig. 3 Four-row (*upper row images*) vs. 16-row (*lower row images*) MDCT ACVB to RCX bypass in the proximal, middle and distal course

Matching our results in LITA to LAD and ACVB to RCX bypasses, the distal anastomosis could not be delineated any better in ACVB to RCA bypasses ($P>0.05$) [(Fig. 4, 4-row vs. 16-row)]. Sixteen-row technology yielded significantly better results in the proximal anastomosis as well as the total, proximal, middle and distal course of ACVB to RCA grafts ($P<0.05$) [(Fig. 5, 4-row vs. 16-row)]. P values for each segment and reformation used are displayed in Table 3.

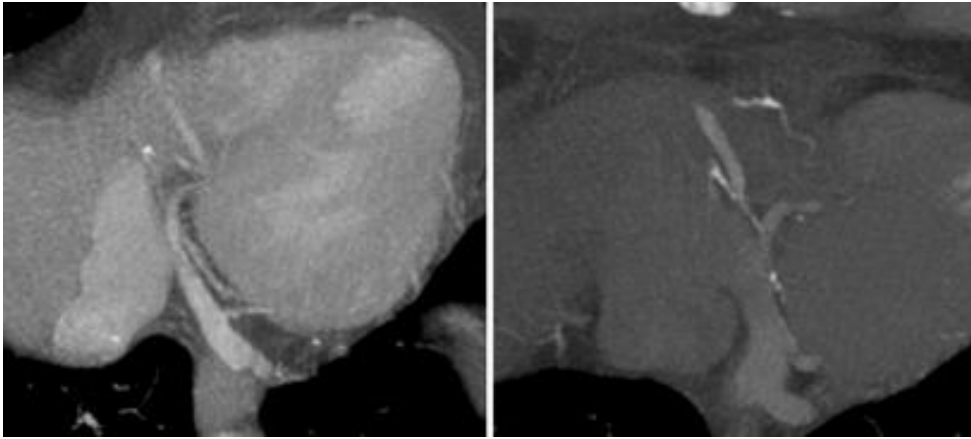


Fig. 4 Four-row (*left image*) vs. 16-row (*right image*) MDCT ACVB to RCA bypass at the distal anastomosis

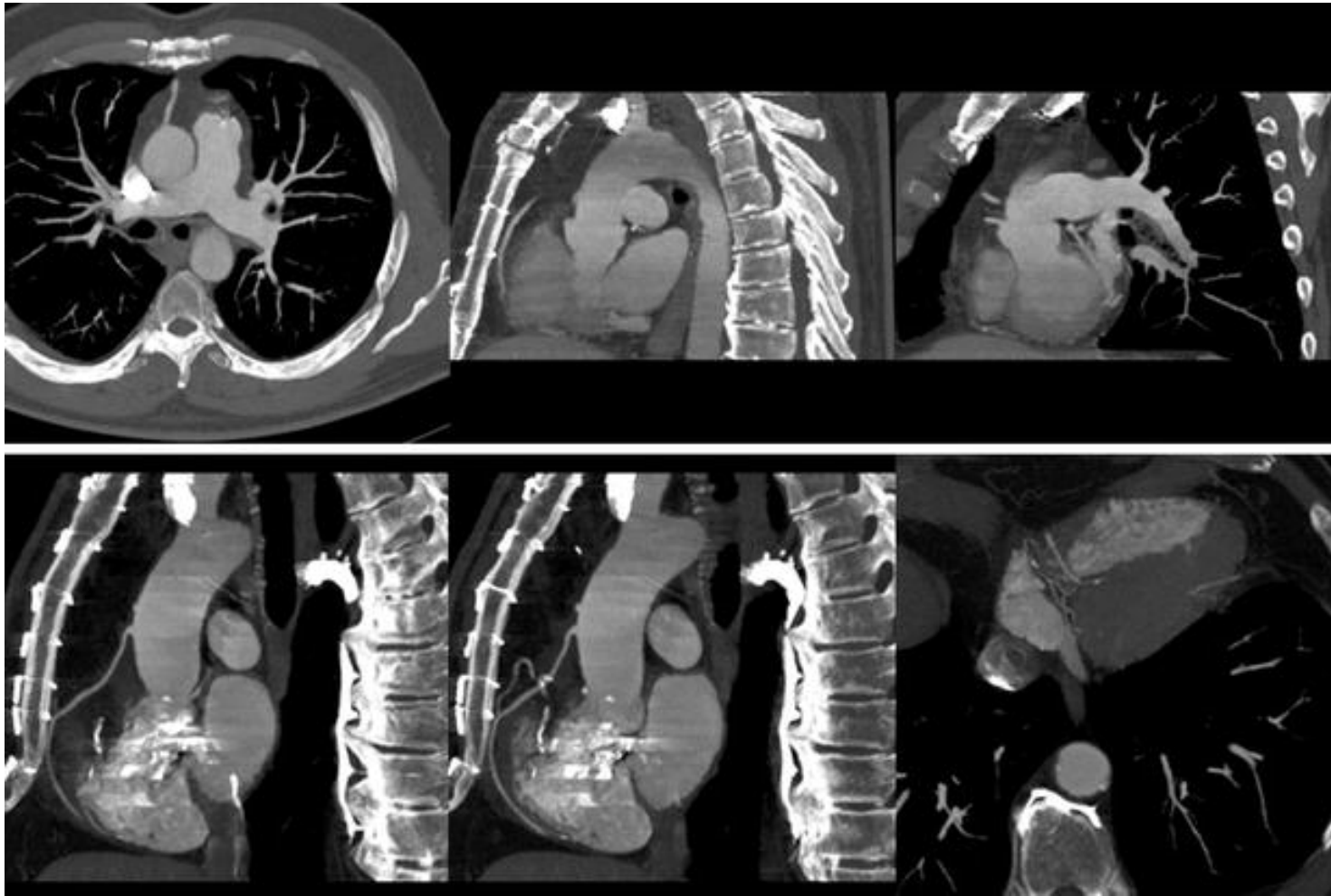


Fig. 5 Four-row (*upper row images*) vs. 16-row (*lower row images*) MDCT ACVB to RCA bypass in the proximal, middle and distal course

Table 3 *P* values for each segment and reformation used comparing 4-row MDCT with 16-row MDCT

Bypass type	Total course			Proximal anastomoses			Proximal course			Middle course			Distal course			Distal anastomoses		
	4-row CT	16-row CT	P value	4-row CT	16-row CT	P value	4-row CT	16-row CT	P value	4-row CT	16-row CT	P value	4-row CT	16-row CT	P value	4-row CT	16-row CT	P value
LITA-LAD																		
MIP thin	2.4 ±1.047	1.873 ±0.963	0.005				2.127 ±0.924	1.709 ±0.916	0.015	2.382 ±1.097	1.8 ±0.989	0.004	2.855 ±0.989	2.227 ±0.904	0.003	2.836 ±1.014	2.545 ±1.152	0.112
MPR	3 ±0.861	2.636 ±0.778	0.04				2.509 ±0.998	2.164 ±0.834	0.04	3.036 ±0.881	2.564 ±0.834	0.004	3.327 ±0.982	2.873 ±0.862	0.007	3.236 ±1.053	3.982 ±0.933	0.142
VRT	2.509 ±1.086	1.891 ±1.012	0.002				2.018 ±1.027	1.473 ±0.94	0.003	2.509 ±1.120	1.745 ±1.058	0.001	3.018 ±1.147	2.309 ±1.184	0.001	3.036 ±1.170	2.829 ±1.329	0.258
ACVB-RCA																		
MIP thin	2.5 ±1.210	2.25 ±1.349	0.026	1.864 ±1.268	1.291 ±0.923	0.032	1.818 ±1.263	1.236 ±1.406	0.042	2.409 ±1.335	2.127 ±1.344	0.042	3.25 ±1.278	2.727 ±1.301	0.042	3.273 ±1.264	3 ±1.364	0.304
MPR	2.682 ±1.095	2.073 ±1.097	0.043	2.136 ±1.173	1.689 ±0.835	0.031	2.227 ±1.198	1.364 ±1.222	0.035	2.682 ±1.157	2.173 ±1.138	0.041	3.273 ±1.208	2.590 ±1.098	0.036	3.25 ±1.241	3.295 ±1.173	0.809
VRT	2.273 ±1.318	1.53 ±1.366	0.033	1.773 ±1.256	1.264 ±0.942	0.036	1.795 ±1.322	1.288 ±1.483	0.02	2.25 ±1.366	1.836 ±1.456	0.007	3 ±1.258	2.563 ±1.463	0.01	3.091 ±1.291	3.364 ±1.399	0.3
ACVB-RCX																		
MIP thin	2.209 ±0.888	1.791 ±1.013	0.046	1.442 ±0.765	1.032 ±0.787	0.026	1.465 ±0.758	1.115 ±0.821	0.045	1.977 ±0.988	1.721 ±1.054	0.031	3.023 ±1.102	2.395 ±1.178	0.024	3.163 ±1.067	2.989 ±1.245	0.119
MPR	2.488 ±0.768	2.042 ±0.854	0.023	1.767 ±0.751	1.261 ±0.756	0.017	1.814 ±0.764	1.023 ±0.74	0.016	2.512 ±0.768	2.119 ±0.906	0.036	3.186 ±1.006	2.884 ±0.851	0.015	3.256 ±1.049	3.047 ±0.975	0.378
VRT	2.395 ±0.979	1.837 ±1.09	0.009	1.442 ±0.796	1.14 ±0.413	0.049	1.488 ±0.91	1.126 ±0.747	0.037	2.07 ±0.985	1.491 ±1.226	0.002	3.419 ±1.239	2.558 ±1.402	0.004	3.535 ±1.241	3.343 ±1.463	0.056

Comparison of reformations within group A and B showed that thin slap maximum intensity projection (MIP thin) [($P < 0.05$)] and volume rendered reformations (VRT) [($P < 0.05$)] displayed better visualization as compared to MPR (Table 4), [(Figs. 6, 7)].

Table 4 *P* value comparison of reformations within groups, 4-row and 16-row MDCT

	Total course		Proximal anastomoses		Proximal course		Middle course		Distal course		Distal anastomoses	
	MPR	VRT	MPR	VRT	MPR	VRT	MPR	VRT	MPR	VRT	MPR	VRT
LITA–LAD												
4-row CT												
MIP thin	0.00004	0.055	0.00084	0.5782	0.000003	0.907275	0.000085	0.189608	0.000025	0.774068	0.00073	0.0821
MPR		0.003		0.000018		0.00037		0.0018		0.00012		0.00056
16-row												
MIP thin	0.000146	0.108783	0.00051	0.68991	0.000856	0.802088	0.000146	0.15744	0.00183	0.407277	0.000171	0.76021
MPR		0.00073		0.00418		0.000189		0.000826		0.000387		0.000983
ACVB–RCA												
4-row CT												
MIP thin	0.000302	0.999569	0.000071	0.951779	0.000353	0.834425	0.000925	0.995859	0.000861	0.9995	0.00038	0.185
MPR		0.0035		0.00051		0.00022		0.000002		0.000302		0.00421
16-row												
MIP thin	0.000643	0.687367	0.00351	0.749678	0.001863	0.927083	0.002607	0.560875	0.000411	0.922947	0.004198	0.2518
MPR		0.000983		0.000055		0.00163		0.00781		0.000004		0.000361
ACVB–RCX												
4-row CT												
MIP thin	0.000013	0.993223	0.000964	0.903245	0.000353	0.834425	0.000458	0.613108	0.000179	0.999987	0.000477	0.7713

MPR		0.00025		0.00047		0.00062		0.000427		0.004059		0.00098
16-row CT												
MIP thin	0.00001	0.328697	0.0031121	0.999364	0.001863	0.927083	0.00014	0.203206	0.000001	0.898188	0.000759	0.0719
MPR		0.00026		0.009279		0.00351		0.000241		0.000459		0.00561

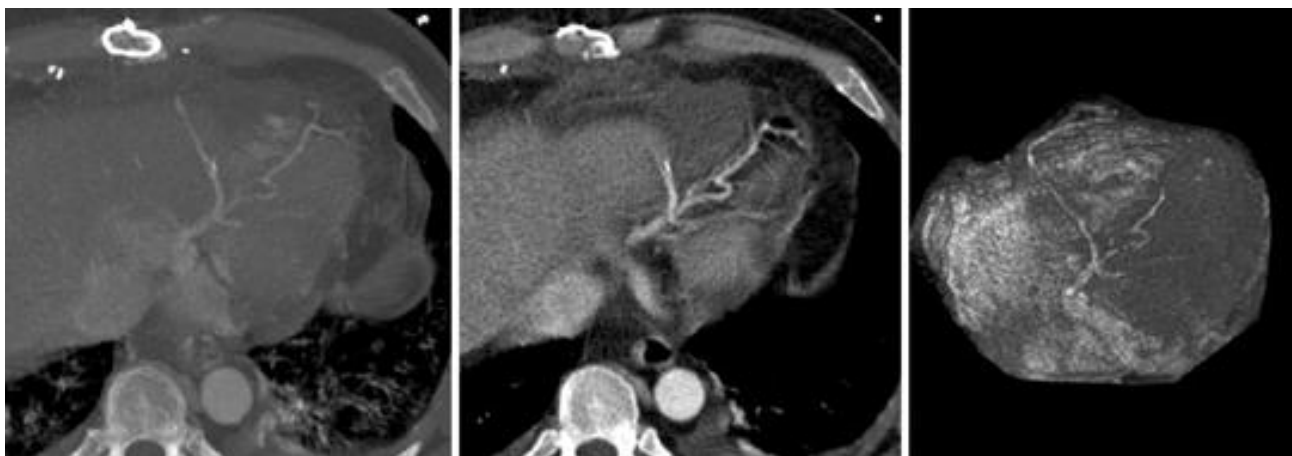


Fig. 6 Comparison of reformations within group A; MIP thin (*left image*), MPR (*middle image*) and volume-rendered reformation (VRT) [(*right image*)]

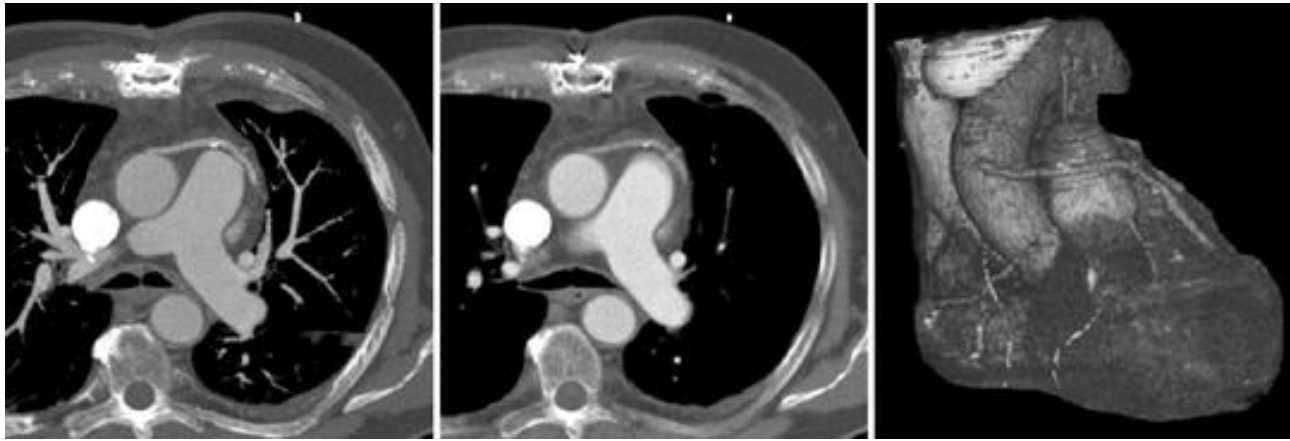


Fig. 7 Comparison of reformations within group B; MIP thin (*left image*), MPR (*middle image*) and volume-rendered reformation (VRT) (*right image*)

Interobserver correlation varied between bypass types, reformations and segment evaluated. For LITA to LAD grafts rho 0.79–0.92. For ACVB to RCx grafts rho 0.74–0.98 and for ACVB to RCA grafts rho 0.71–0.95. Correlations are listed in detail in Table [5](#).

Table 5 Interobserver correlation

	Total course	Proximal anastomoses	Distal anastomoses
4-row CT			
MIP thin	0.809/0.922/0.824	×/0.753/0.926	0.848/0.882/0.789
MPR	0.900/0.949/0.888	×/0.711/0.755	0.897/0.813/0.920
VRT	0.882/0.926/0.867	×/0.747/0.957	0.884/0.920/0.928
16-row CT			
MIP thin	0.827/0.923/0.980	×/0.817/0.761	0.789/0.843/0.898

MPR	0.81/0.807/0.772	×/0.741/0.953	0.884/0.943/0.844
VRT	0.787/0.792/0.744	×/0.731/0.734	0.915/0.952/0.923

LITA to LAD/ACVB to RCA/ACVB to RCX.

Discussion

Since the introduction of cardiac CT angiography in the late 1990s and with it the evaluation of bypass grafts using MDCT technology [22, 23], authors benchmarking the relatively new method with angiography, the current gold standard, have expressed their confidence that future generations of multidetector technology will bridge the gap to the gold standard [6, 7, 24].

In patients after bypass surgery, invasive angiography often is an underestimated challenge due to degenerated and diffusely calcified vessels. In cases of complex revascularization, the anatomy of the grafts is often very confusing and the exact knowledge of number and type of grafting performed is very useful. A non-invasive approach adds up to the complexity of the situation.

As the quality of cardiac CT angiography desperately relies on the reduction of respiratory and cardiac motion artifacts, using 16-row technology with faster scan time and temporal resolution up to 110 ms as well as nearly isotropic voxel size with a slice thickness of <1 mm can be of no harm. The reduction in scan time in 16-row technology by half allows visualization of the LITA to LAD grafts in almost their entire course, without the use of preoxygenation [25]. It is evident that the probability of motion artifacts caused by breathing is reduced by a shorter scan time. Especially assessment of the distal anastomosis is a problem that has been neglected in the recent past because of technical limitations and commonly has been deflected to being addressed in future MDCT generations [8].

Still, vascular metal clips, particularly along the course of vessels with smaller diameters such as arterial grafts, are prone to beam hardening and partial volume effects that may hinder proper assessment [26]. However, sensitivities between 76 and 100% and specificities between 92 and 98% have been described by several authors, depending on the evaluation of graft occlusion or substantial graft stenosis [24, 27, 28].

Our data report that 16-row MDCT technology in comparison to 4-row MDCT technology yielded a better assessment of the proximal anastomosis, the proximal, middle, distal course and total course of the graft vessel, no matter which kind of grafting was performed (Table 3).

We can confirm the experience of Nieman et al. [24] that thin-slab MIPs were the best algorithm to assess an extended length of a bypass. In the presence of metal clips, the use of MIP resulted in over projection in which case evaluation was continued using multiplanar reconstruction or transverse sections. Volume-rendering technique was used for global orientation and presentation of results. In cases of complex revascularization in which the number and type of bypass grafts were sometimes largely unknown, it is very useful to get an overview of the bypass anatomy first using VRT before starting evaluation of the patency and image quality of each segment. This is particularly useful when outpatients are subject to examination and there is only limited information obtainable from the patient or the referring physician. However, neither VRT nor any other reformation we examined can detect grafts with total occlusion in the proximal anastomosis. Therefore, a precise patient history and detailed information on the grafting performed is crucial for a proper evaluation. Dewey et al. report on 75 bypass grafts they evaluated, of which 99% of the distal anastomoses were described as eligible for assessment [29]. However, in our results visualization of the distal anastomosis was equal in both groups. Though a clear trend towards enhanced bypass visualization can be reported, one should keep clearly in mind that visualization of the distal anastomosis did not display any improvement.

Despite better temporal resolution, shorter scan time and a smaller collimation, we cannot report on better results for the evaluation of the distal anastomosis using 16-row technology. To some extent, this can be attributed to the fact that both groups had to cope with patients in whom heart rates much above the optimum of 60 bpm were observed. Although beta-blockers were routinely administered to all patients with HR >70 bpm prior to examination, the mean heart rate was as high as 83 bpm for patients in group B (16-row MDCT). In the context of cardiac CT examinations, whether administration of beta-receptor blocking medication in patients with severe cardiac limitations and medication is useful should be discussed. The lack of validation of our results with coronary angiography would have been a limitation if bypass patency had been the main issue of this study. Instead, the focus was on the relative improvement in 16-row MDCT vs. 4-row MDCT, in which case we think a correlation with coronary angiography is not necessarily required. Plaque formation was not observed and is not commonly expected in patients shortly after surgery.

Sixteen-row technology may fall short in the needs and expectations in respect to distal anastomoses, but the next generation of multidetector CT scanners with an increased temporal resolution using faster rotating X-ray tubes and a smaller collimation may enable us to assess the distal parts of bypass grafts.

References

1. Bruckenberg E (2001) Bericht der Arbeitsgruppe Krankenhauswesen der Arbeitsgemeinschaft der obersten Landesgesundheitsbehörden der Länder (AOLG). Herzbericht 14:2001

2. Berger PB, Alderman EL, Nadel A, Schaff HV (1999) Frequency of early occlusion and stenosis in a left internal mammary artery to left anterior descending artery bypass graft after surgery through a median sternotomy on conventional bypass: benchmark for minimally invasive direct coronary artery bypass. *Circulation* 100:2353–2358

[ChemPort](#)[PubMed](#)

3. Tan ES, van der Meer J, Jan de Kam P et al (1999) Worse clinical outcome but similar graft patency in women versus men one year after coronary artery bypass graft surgery owing to an excess of exposed risk factors in women. CABADAS. Research Group of the Interuniversity Cardiology Institute of The Netherlands. Coronary artery bypass graft occlusion by aspirin, dipyridamole and acenocoumarol/phenoprocoumon study. *J Am Coll Cardiol* 34:1760–1768

[crossref](#)[ChemPort](#)[PubMed](#)

4. Serruys PW, Unger F, Sousa JE et al (2001) Comparison of coronary-artery bypass surgery and stenting for the treatment of multivessel disease. *N Engl J Med* 344:1117–1124

[crossref](#)[ChemPort](#)[PubMed](#)

5. Goldman S, Zadina K, Krasnicka B et al (1997) Predictors of graft patency 3 years after coronary artery bypass graft surgery. Department of Veterans Affairs Cooperative Study Group No. 297. *J Am Coll Cardiol* 29:1563–1568

[crossref](#)[ChemPort](#)[PubMed](#)

6. von Smekal A, Lachat M, Wildermuth S, Khan G, Turina M, Marincek B (2000) Proximal anastomoses of aortocoronary bypasses. Evaluation with ECG-triggered single-slice computerized tomography. *Radiologe* 40:130–135

[\[SpringerLink\]](#)[PubMed](#)

7. Kwok BW, Lim TT (2000) Cortical blindness following coronary angiography. *Singapore Med J* 41:604–605

[ChemPort](#)[PubMed](#)

8. Silber S, Finsterer S, Kruschke I, Lochow P, Muhling H (2003) Noninvasive angiography of coronary bypass grafts with cardio-CT in a cardiology practice. *Herz* 28:126–135

[\[SpringerLink\]](#)[PubMed](#)

9. Marano R, Storto ML, Maddestra N, Bonomo L (2004) Non-invasive assessment of coronary artery bypass graft with retrospectively ECG-gated four-row multi-detector spiral computed tomography. *Eur Radiol* 14:1353–1362

10. Cademartiri F, Mollet N, van der Lugt A et al (2004) Non-invasive 16-row multislice CT coronary angiography: usefulness of saline chaser. *Eur Radiol* 14:178–183



11. Ohnesorge B, Flohr T, Becker C et al (2000) Cardiac imaging with rapid, retrospective ECG synchronized multilevel spiral CT. *Radiologe* 40:111–117



12. Ohnesorge B, Flohr T, Becker C et al (2000) Cardiac imaging by means of electrocardiographically gated multisection spiral CT: initial experience. *Radiology* 217:564–571



13. Flohr T, Ohnesorge B (2001) Heart rate adaptive optimization of spatial and temporal resolution for electrocardiogram-gated multislice spiral CT of the heart. *J Comput Assist Tomogr* 25:907–923



14. Luisada AA, MacCanon DM (1972) The phases of the cardiac cycle. *Am Heart J* 83:705–711



15. Herzog C, Dogan S, Diebold T et al (2003) Multi-detector row CT versus coronary angiography: preoperative evaluation before totally endoscopic coronary artery bypass grafting. *Radiology* 229:200–208



16. Achenbach S, Ropers D, Holle J, Muschiol G, Daniel WG, Moshage W (2000) In-plane coronary arterial motion velocity: measurement with electron-beam CT. *Radiology* 216:457–463



17. Hong C, Becker CR, Huber A et al (2001) ECG-gated reconstructed multi-detector row CT coronary angiography: effect of varying trigger delay on image quality. *Radiology* 220:712–717



18. Kopp AF, Ohnesorge B, Flohr T et al (2000) Cardiac multidetector-row CT: first clinical results of retrospectively ECG-gated spiral with optimized temporal and spatial resolution. *Rofo Fortschr Geb Rontgenstr Neuen Bildgeb Verfahr* 172:429–435



19. Georg C, Kopp A, Schroder S et al (2001) Optimizing image reconstruction timing for the RR interval in imaging coronary arteries with multi-slice computerized tomography. *Rofo Fortschr Geb Rontgenstr Neuen Bildgeb Verfahr* 173:536–541



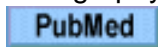
20. Rodenwaldt J (2003) Multislice computed tomography of the coronary arteries. *Eur Radiol* 13:748–757



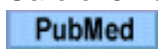
21. Nikolaou K, Sagmeister S, Knez A et al (2003) Multidetector-row computed tomography of the coronary arteries: predictive value and quantitative assessment of non-calcified vessel-wall changes. *Eur Radiol* 13:2505–2512



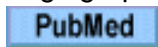
22. Lu B, Dai RP, Zhuang N, Budoff MJ (2002) Noninvasive assessment of coronary artery bypass graft patency and flow characteristics by electron-beam tomography. *J Invasive Cardiol* 14:19–24



23. Pasowicz M, Klimeczek P, Pieniazek P et al (2002) Assessment of stent patency using multi-slice spiral computed tomography: initial experience. *Acta Cardiol* 57:63–64



24. Nieman K, Pattynama PM, Rensing BJ, Van Geuns RJ, De Feyter PJ (2003) Evaluation of patients after coronary artery bypass surgery: CT angiographic assessment of grafts and coronary arteries. *Radiology* 229:749–756



25. Enzweiler CN, Kivelitz DE, Wiese TH et al (2000) Coronary artery bypass grafts: improved electron-beam tomography by prolonging breath holds with preoxygenation. *Radiology* 217:278–283



26. Knollmann FD, Moller J, Gebert A, Bethge C, Felix R (2004) Assessment of coronary artery stent patency by electron-beam CT. *Eur Radiol* 14:1341–1347



27. Achenbach S, Moshage W, Ropers D, Nossen J, Bachmann K (1997) Noninvasive, three-dimensional visualization of coronary artery bypass grafts by electron beam tomography. *Am J Cardiol* 79:856–861



28. Ropers D, Ulzheimer S, Wenkel E et al (2001) Investigation of aortocoronary artery bypass grafts by multislice spiral computed tomography with electrocardiographic-gated image reconstruction. *Am J Cardiol* 88:792–795



29. Dewey M, Lembcke A, Enzweiler C, Hamm B, Rogalla P (2004) Isotropic half-millimeter angiography of coronary artery bypass grafts with 16-slice computed tomography. *Ann Thorac Surg* 77:800–804

